Proceedings of ASME Turbo Expo Turbine Technical Conference
IGTI 2011
June 6-10, 2011, Vancouver, Canada

GT2011-46359

TIP CLEARANCE INVESTIGATION OF A DUCTED FAN USED IN VTOL UAVS

PART 2: NOVEL TREATMENTS VIA COMPUTATIONAL DESIGN AND THEIR EXPERIMENTAL VERIFICATION

Ali Akturk[*]
Turbomachinery Aero-heat Transfer Laboratory
Department Aerospace Engineering
The Pennsylvania State University
University Park, Pennsylvania 16802
Email: aua162@psu.edu

Cengiz Camci [†]
Turbomachinery Aero-heat Transfer Laboratory
Department Aerospace Engineering
The Pennsylvania State University
University Park, Pennsylvania 16802
Email: cxc11@psu.edu

ABSTRACT

Ducted fan based vertical lift systems are excellent candidates to be in the group of the next generation vertical lift vehicles, with many potential applications in general aviation and military missions. Although ducted fans provide high performance in many "Vertical Take-Off and Landing" (VTOL) applications, there are still unresolved problems associated with these systems. Fan rotor tip leakage flow adversely affects the general aerodynamic performance of ducted fan VTOL UAVs. The current study utilized a three dimensional Reynolds-Averaged Navier Stokes (RANS) based CFD model of ducted fan for the development and design analysis of novel tip treatments. Various tip leakage mitigation schemes were introduced by varying the chordwise location and the width of the extension in the circumferential direction. Reduced tip clearance related flow interactions were essential in improving the energy efficiency and range of ducted fan based vehicles. Full and inclined pressure side tip squealers were also designed. Squealer tips were effective in changing the overall trajectory of the tip vortex to a higher path in radial direction. The interaction of rotor blades and tip vortex was effectively reduced and the aerodynamic performance of the rotor blades was improved. The overall aerodynamic gain was a measurable reduction in leakage mass flow rate. This leakage reduction increased thrust significantly. Experimental measurements indicated that full and inclined pressure side tip squealers increased thrust obtained in hover condition by 9.1 % and 9.6 % respectively. A reduction or elimination of the momentum deficit in tip vortices is essential to reduce the adverse performance effects originating from the unsteady and highly turbulent tip leakage flows rotating against a stationary casing. The novel tip treatments developed throughout this study are highly effective in reducing the adverse performance effects of ducted fan systems developed for VTOL UAVs.

NOMENCLATURE

c Chord length
C_p Static pressure coefficient
C_{pt} Total pressure coefficient, $C_{pt} = \frac{P_{te}-P_{ti}}{\frac{1}{2}\rho U_m^2}$
C_P Power coefficient, $C_P = \frac{\text{Power}}{\rho\omega^3 D^5}$
C_T Thrust coefficient, $C_T = \frac{\text{Thrust}}{\rho\omega^2 D^4}$
D Shroud (casing) inner diameter (m)
ε Relative error calculated wrt experimental values
h Blade height
θ Circumferential position
p Static pressure
PS Pressure side
R Ideal gas constant,(for air $R = 287\ \frac{J}{Kg \cdot K}$)
RANS Reynolds-Averaged Navier Stokes

[*]Postdoctoral Research Fellow
[†]Professor of Aerospace Engineering, corresponding author

sh Squealer height
SS Suction side
t Effective tip clearance in inches
t.p.e. Tip platform extentions
t/h Relative tip clearance wrt blade height
UAV Uninhabited Aerial Vehicles
$VTOL$ Vertical Take-Off and Landing
y^+ Non-dimensional wall distance
w Squealer width

INTRODUCTION

Ducted fan designs require large tip clearances in order to safely operate in VTOL UAVs. The large tip clearance induced flow has a damaging effect on the fan rotor aerodynamic performance. It is also a significant energy loss mechanism in the ducted fans.

This paper describes the development of novel tip treatments for ducted fans used in VTOL UAVs. Ducted fan VTOL UAVs use large tip gaps because of their operating conditions. Large tip clearance flow increases the aerodynamic losses on the fan rotor and diminish the performance of the ducted fan. Novel tip treatments are aimed to reduce the losses and improve performance.

There has been a limited number of studies about three dimensional flow structure of leakage vortex in axial flow fans and compressors, in open literature [1–5]. Inoue and Kuroumaru et al. [6] made detailed flow measurements before and behind an axial flow rotor with different tip clearances. In their study, they investigated the clearance effect on the behavior of tip leakage flow. Furukawa and Inoue et al. [7] also investigated breakdown of tip leakage vortex in a low speed axial flow compressor. Reducing tip leakage mass flow rate improves the aerodynamic performance of axial flow fans and compressors. Implementation of treatments in the non-rotating part over the blade tip is also an efficient way of tip leakage flow reduction. References [8] and [9] investigate different casing treatments for axial flow compressors.

A few authors investigated tip treatments in turbomachinery components for tip leakage mass flow reduction. Corsini et al. [10–14] presented the results of a computational study of an axial flow fan using "*improved tip concepts*". The first two endplates were with constant and variable thickness distributions while the last two were designed by combining the end-plates with a stepped gap on the tip. The investigation was based on a finite element Navier-Stokes solver for the physical interpretation of the detailed 3D leakage flow field. The specific fan performance experiments showed that the improved tip concepts introduced a small performance penalty, but the efficiency curves give evidence of an improvement with better peak performance and a wider high efficiency curve towards the rotor stall margin. An aeroacoustic investigation showed a reduction of the rotor aeroacoustic signature.

Wisler [15] presented a study on tip clearance and leakage effects in compressors and fans. He discussed the effect of clearance, duct design, tip treatments, active clearance control, and improving stall margin of rotor blade in his study. He came up with several tip treatment geometries. He has tested squealer tip, groove, pressure and suction side winglet, knife type tip configurations. The most common one of these treatments is the squealer tip obtained by thinning the rotor tip. The main reason for a squealer tip is the reduction of the contact surface during a "*rubbing*" incidence. A squealer tip has measurable aerodynamic benefits too. Relative to flat tip the deep groove treatment and the pressure surface winglet implementation reduced the leakage.

Akturk and Camci [16] developed novel tip platform extensions for energy efficiency gains and aeroacoustic improvements for a constant rotational speed axial flow fan. They have measured three components of velocity at downstream of the fan rotor for five different tip platform extensions, introduced on the pressure side of the fan rotor tip section. They have showed that the tip platform extensions have proven to be effective swirl reducing devices at the exit of the fan. The magnitude of this reduction is about one third of the rotor exit velocity magnitude in the core of the passage exit. Their results also showed that the mean kinetic energy of fan exit flow increased due to the increase in mean axial velocity.

Martin and Boxwell [17] tested two ducted fan models that were designed to effectively eliminate the tip leakage. Both models were derived from the baseline (10-inch inner-diameter shroud) which is explained in their previous study [18]. In their fist design, they have created a notch and fit the propeller inside the notch. In their second design, a rearward-facing step was cut into the inner shroud. The computational analysis resulted in an increase in inlet lip suction and an increase in performance. However, the experimental thrust and power measurements, showed no difference in performance of these designs when compared to their baseline duct.

Novel tip platform extensions for aerodynamic and aeromechanic improvements were designed in the current investigation for a ducted fan VTOL UAV in hover condition. Five tip treatments were developed by using numerical solutions of Reynolds Averaged Navier-Stokes equations. Selected computationally developed tip trea treatments were also experimentally verified in the 22" ducted fan test bench. Fan rotor downstream total pressure surveys, force and moment measurements were performed. The main goal of this paper is to develop effective tip treatments for reducing tip leakage flow for large tip gaps used in ducted fans for VTOL UAVs. This paper presents a set of comprehensive ducted fan aerodynamic measurements validating and supporting the computationally developed novel tip treatments named full and partial bump tip extensions, full bump and partial squealar tip extensions, and full squealer and inclined squealer tips in hover condition. A comprehensive assessment and validation of the computational method used in this paper was ex-

plained in an accompanied paper by Akturk and Camci [19].

DESIGN ALGORITHM OF TIP TREATMENTS

Computational Method

A three dimensional computational method can be used to develop novel tip treatments for improving aerodynamic performance of the ducted fan in hover.

Reynolds averaged Navier-Stokes solutions were obtained for computational analysis by using Ansys-CFX. The computational analysis for the tip treatment development was performed on three different computational domains that are connected. The details of the computational method, computational domain sections, grid implementation and boundary conditions used in this paper can be found in an accompanying paper by Akturk and Camci [19]. Inlet section includes an inlet lip surface that was considered as a solid wall with no-slip condition. Atmospheric static pressure was prescribed on the top surface. On the side surface, an opening type boundary condition was assumed.

The outlet section includes the outer duct surface, circular rods, rotor hub surface and support structure underneath of the system that is considered as solid walls with no-slip condition. Bottom surface is also treated with no -slip boundary condition. On the side surface, an opening boundary condition is assumed.

The rotating section includes the fan blades, rotor hub region and shroud surface. The rotating fluid motion at a constant angular velocity is simulated by adding source terms to the Navier-Stokes equations for the effects of the Coriolis force and the centrifugal force. Counter rotating wall velocities are assigned at the shroud surface.

Stationary and rotating regions were sub-sectional by periodic surfaces. By the help of periodicity, speed of numerical simulations were increased. The stationary surfaces were divided into 4 segments, and the rotating region was divided into 8 periodic segments. Only one of these segments for each region was used in numerical calculations. Difference in pitch angles of the frames is taken into account in interfaces that are connecting rotating and stationary surfaces. A stage type interface model was used.

The stage model performs a circumferential averaging of the fluxes on the interface surface. This model allows steady state predictions to be obtained for turbomachinery components. The stage averaging at the frame change interface introduces one-time mixing loss. This loss is equal to assume the physical mixing supplied by the relative motion between stationary and rotating surfaces. General grid interface (GGI) is used for mesh connections between interfaces.

Figure 1 illustrates a view from medium size computational mesh near the squelar and inclined squelar rotor tips. Non-dimensional wall distance (y^+) less than 2 is achieved near the shroud, rotor tip and treatment surfaces.

The numerical simulations for tip treatments were obtained at 2400 rpm rotor speed for hover condition. Calculations were performed using a parallel processing approach. For the parallel processing, the stationary and rotating frames were partitioned via vertex based partitioning with metis multilevel k-way algorithm. Computations were performed on a cluster having 24 processors. Total processing time is approximately 54.9 hours. The flow within the computational domain was initialized as no flow at the freestream static conditions. The convergenced solution was achieved approximately within 4500 iterations. The (root mean square) RMS residuals of the Navier-Stokes equations were compared for judging convergence.

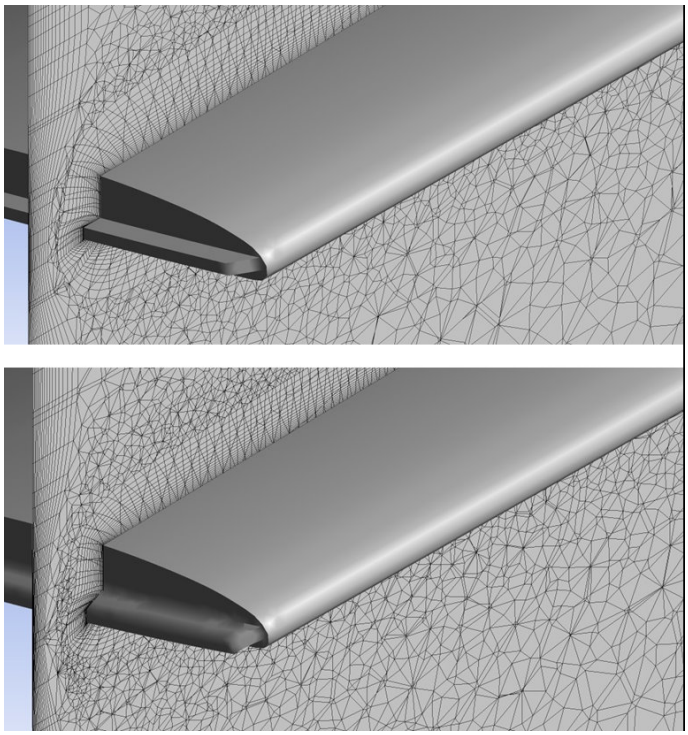

FIGURE 1. The near tip computational grid for squealar and inclined squealer rotor tips

Blade tip constant circumferential angle planes

The visualization planes obtained at constant circumferential angles are generated at the rotor blade tip for a better understanding of the rotor tip region flow. They are all passing from the axis of rotation and drawn at fixed circumferential position (θ). Three of these planes (A,B and C) were drawn just upstream of the rotor tip and they are seperated by 4^o circumferential angle from each other and plane D. Plane D was drawn at the quarter chord of the tip profile. Planes D, E,F,G,H and I were equally distributed near the rotor tip profile by 2^o circumferential angle increments. Plane I was drawn at the trailing edge.

Constant circumferential angle planes drawn in Figure 2

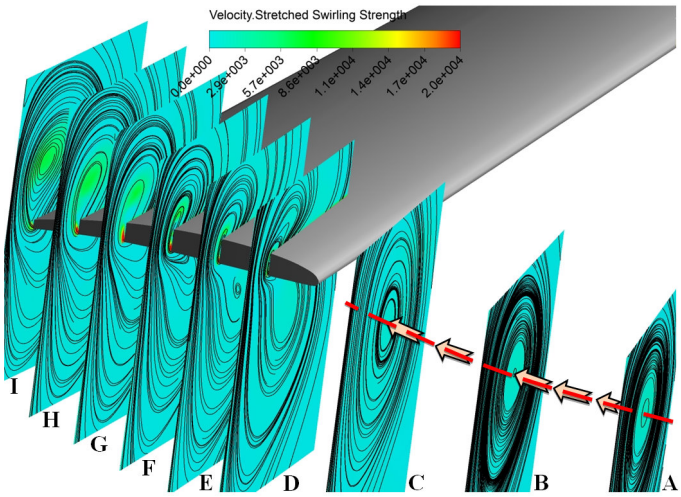

FIGURE 2. Blade tip constant circumferential angle planes drawn for baseline rotor tip with 3.04 % tip clearance

are colored with the magnitude of stretched swirling strength. Swirling strength is the imaginary part of complex eigenvalues of velocity gradient tensor. It is positive if and only if there is existence of a swirling local flow pattern and its value represents the strength of swirling motion around local centers. Stretched swirling strength is swirling strength times dot product of swirling vector and normal of swirling plane. An increase in this parameter indicates that swirling strength normal to swirling plane is increased.

The quantity color coded in these planes is the velocity stretched swirling strength drawn on the constant circumferential angle planes. The swirling strength shows the magnitude of the out of plane swirling motion. The red color indicates a region that the highest swirling motion is occurring. Plane A, B and C shows swirling strength upstream of the rotor blade. A small amount of swirling motion can be observed in these planes which is related to the tip vortex originating from the previous blade. The positioning of each tip vortex influencing the neighboring blade is clearly shown in the first part of this paper [19]. The vortical field originating from the previous blade tip vortex interacts with the blade tip. This vortical field is divided into two parts as suction side and pressure side parts. The suction side part is integral with the tip vortex of the current blade. The pressure side part interacts with the pressure side of the rotor blade and generates additional loss at the exit plane which is shown in the first part of this paper. The strongest swirling motion starts at the quarter chord of the blade tip measured from the leading edge. Leakage flow tries to pass to suction side by generating a vortical structure which is visible at plane D. In planes E,F,G,H and I path of the released vortical structure from the pressure side corner can be viewed. Once the vortical structure forms, the strength of it is not as high as the one observed near the pressure side corner seen in plane D. The size of the flow structure dominated by light blue and green zones is increasing when one travels from the leading edge to trailing edge.

TIP TREATMENT GEOMETRIES

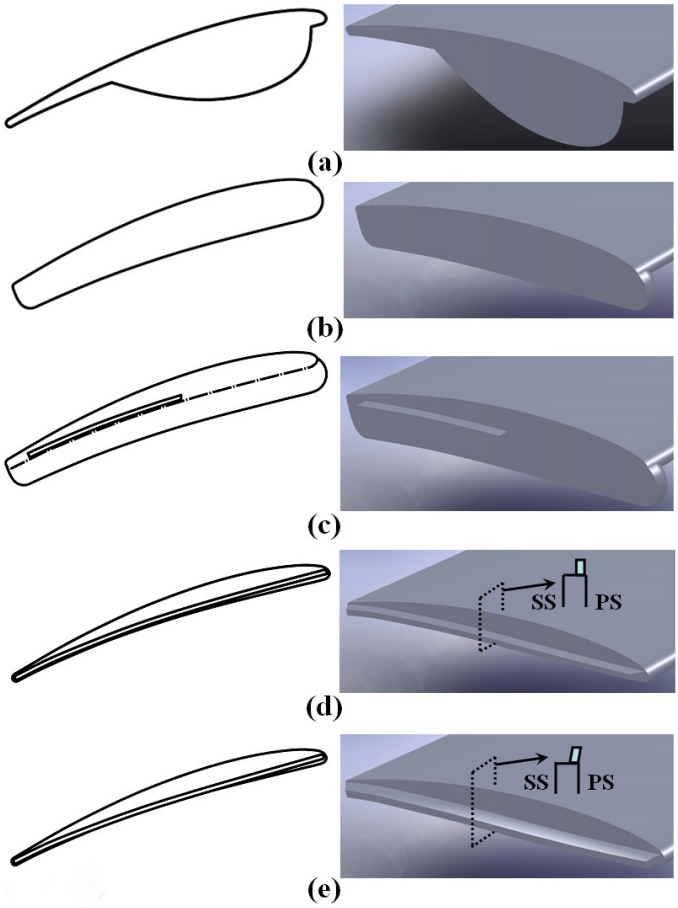

FIGURE 3. Tip treatments (a) Partial bump tip platform extension (t.p.e.), (b) Full bump t.p.e., (c) Full bump and partial squealer t.p.e., (d) Full squealer t.p.e., (e) Inclined full squealer t.p.e.

Tip leakage flow results in a considerable amount of aerodynamic loss in rotor flow field as discussed in previous sections. One way of reducing tip losses is to use proper tip treatments. The specific tip treatments subject to investigation in this paper include special extensions of rotor tip platform and squealer tips. Both types of tip treatments are widely used in axial flow fans and compressors. Figure 3 shows the tip platform extension concepts and squealer tip concepts, that are subject to investigation in this section.

Partial Bump Tip Platform Extension

Effectiveness of partially blocking pressure side of the fan rotor tip in mitigating tip leakage was explained by Akturk and Camci [16]. It was shown that profiles 1 and 2 which are using partial bump type tip platform extension at the pressure side of the fan rotor tip were the best choices for reducing the effects of tip leakage and improving axial flow velocity at the rotor downstream for the lightly loaded fan rotor. Those two bump profiles were having the same thickness with the rotor tip profile at the bump center location. The bump thickness was measured in the circumferential plane at a constant radial position.

The partial bump designed for the current VTOL UAV ducted fan shares the same idea; *reducing the tip leakage flow originating from the pressure side corner of the blade tip*. Computational investigations for the baseline fan rotor with 3.04 % tip clearance discussed in the first part of this paper showed that the tip leakage starts very close to the leading edge of the tip profile. Therefore, a long bump starting from the 5 % of chord location and ending at 66.6 % tip chord location was designed. The maximum thickness point was selected as the quarter chord (25 % of the tip chord) since the highest swirling strength was observed in that location. The maximum thickness of the bump was chosen as "*twice of the tip chord thickness*" at the quarter chord location. Figure 3a shows the shape of the bump designed.

Figure 4 shows streamlines and stretched swirling strength contour for partial bump tip extension shown in Figure 3a. Planes A,B and C are showing tip vortex coming from the previous blade moving radially inward compared to the baseline tip result. The strongest contribution to tip vortex is near plane G. However a gradual increase in the swirling strength is observed in planes D,E and F. Tip vortex can be seen in planes G, H and I with a light green and blue core. Strength of the vortex is slightly higher than the ones obtained for the baseline tip.

Full Bump Tip Platform Extension

Since the leakage flow cannot be effectively blocked by using partial bump tip extension, a full coverage bump tip platform extension was designed to cover the pressure side of the rotor tip completely. The bump starting from the leading edge and ending at the trailing edge of the tip chord was designed. Bump is created by extending pressure side curvature by the airfoil thickness at the quarter chord point of the blade profile. Figure 3b shows the shape of the full bump designed.

Figure 5 shows the streamlines and stretched swirling strength contour for full bump tip extension. Planes A,B and C are showing tip vortex coming from the previous blade moved more axially compared to the baseline tip and the partial bump result. Full bump tip extension was not sufficient for effectively reducing the leakage flow. Planes D,E,F,G,H and I shows that the strength of the vortical structure is almost same with the baseline rotor tip, without a beneficial tip mitigation influence.

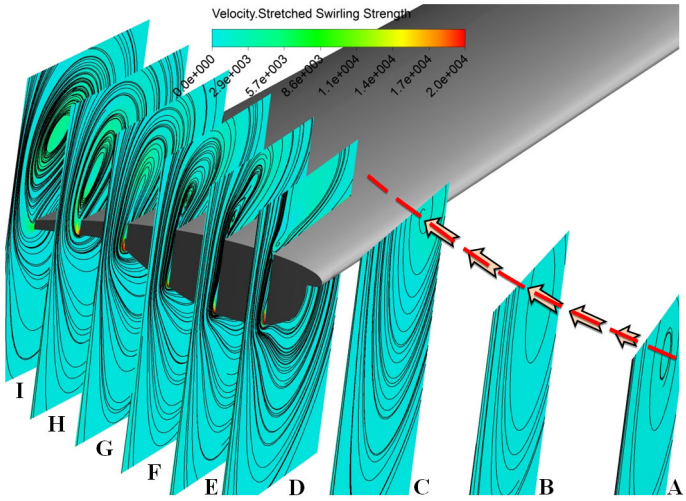

FIGURE 4. Blade tip constant circumferential angle planes drawn for "*partial bump*" tip extension with 3.04 % tip clearance

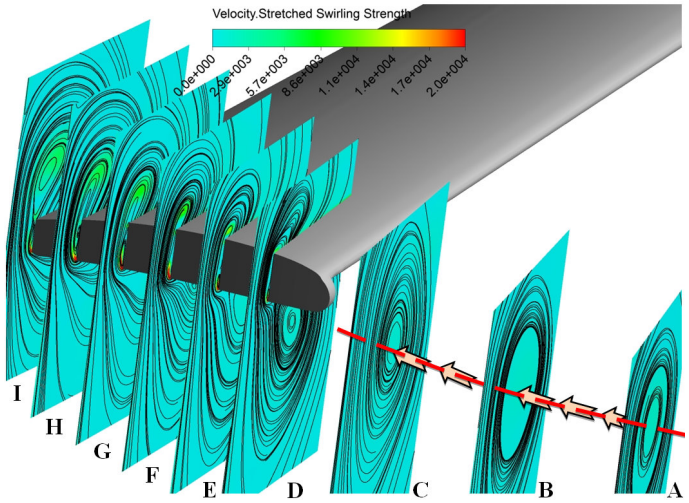

FIGURE 5. Blade tip constant circumferential angle planes drawn for "*full bump*" tip extension with 3.04 % tip clearance

Full Bump and Partial Squealer Tip Platform Extension

Since the leakage flow cannot be properly blocked by using only pressure side tip extensions, a combination of a full bump and a partial squealer extension is designed for the region near the trailing edge. Figure 3c shows the shape of the combined full bump and partial squealer design. The squealer extension starts from 45 % chord measured from leading edge and ends at the trailing edge. The height of the squealar is 0.89 mm and thickness is 20 % of the tip gap height (1.27 mm for 3.04 % tip clearance). The squealar tip is located parallel to the pressure side of the rotor tip and approximately 0.5 mm away from the pressure side.

Figure 6 shows streamlines and stretched swirling strength

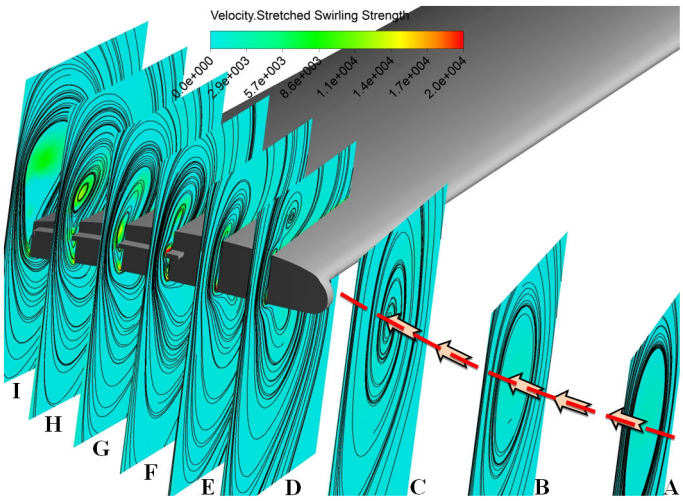

FIGURE 6. Blade tip constant circumferential angle planes drawn for "*full bump and partial squealer*" tip extension with 3.04 % tip clearance

contour for combination of the full bump and squealer tip extension. Planes A,B and C are showing tip vortex coming from the previous blade moving more axially compared to baseline tip and partial bump result. Full bump and squealer tip extension was not sufficient for blocking leakage flow. Planes F,G,H and I shows the effect of squealer on the flow field near the rotor tip. By the effect of the squealar the swirling strength is increased and tip vortex is moved radially outward which is a favorable effect. Moving the tip vortex radially out will reduce the interactions between the tip vortex and rotor blade and reduce the losses. However, the combination of full bump and partial squealer is increasing swirling strength and losses.

Full Squealer Tip Platform Extension Using a combination of bump and squealer is increasing turbulence and swirl at the rotor tip as shown in the previous section. A full squealer tip extension is designed to explore its potential as a possible aerodynamic tip mitigation device. Figure 3d shows the shape of the full squealer tip designed for this. Squealer extension starts from the leading edge of the rotor tip and ends at the trailing edge. The width of the squealer was 0.89 mm and height was 20 % of the tip gap height (1.27 mm for 3.04 % tip clearance). The squealar tip is located parallel to the pressure side of the rotor tip and 0.5 mm away from pressure side. At the leading edge of the tip profile, it is aligned with the stagnation point of the tip profile. Figure 7 shows a sketch of full and inclined squealers.

Figure 8 shows streamlines and stretched swirling strength contour for full squealer tip extension. Squealer tip extension

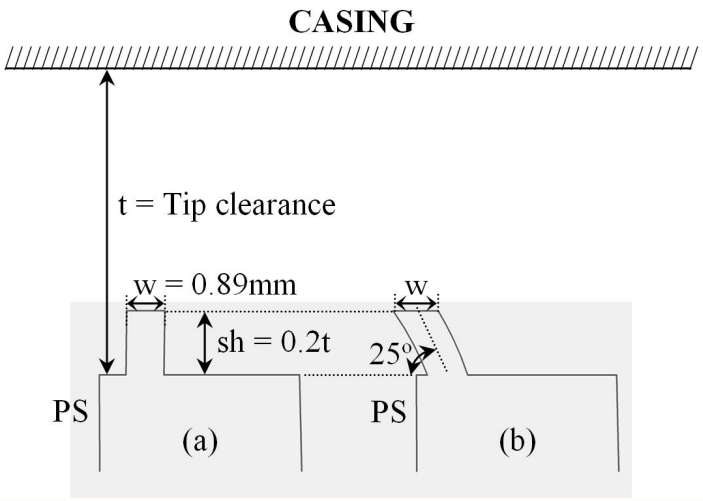

FIGURE 7. (a) Full and (b) inclined squealer sketch

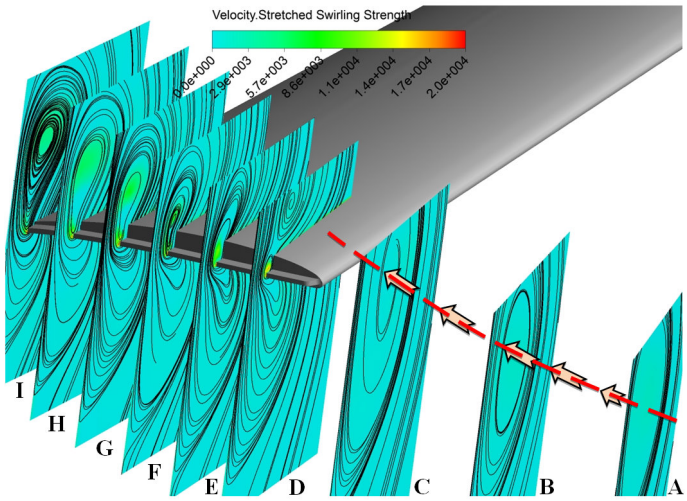

FIGURE 8. Blade tip constant circumferential angle planes drawn for "*full squealer*" tip extension with 3.04 % tip clearance

decreased the strength of swirling at planes D, E, F, G, H and I. The leakage flow starting from the pressure side rolled up a small vortical structure between the squealer and suction side. After plane F, the vortical structure appears on the suction side of the rotor tip. Tip vortex starts to influence the passage flow beginning plane F. Using a squealer tip also moves tip vortex closer to the shroud and relieves the rotor passage from the adverse effect of tip vortex dominated flow. By that way interaction of tip vortex and rotor tip is reduced and rotor tip is loaded better than the baseline rotor tip, because of improvements in the passage aerodynamics near the tip.

Inclined Full Squealer Tip Platform Extension Using the full squealer tip design moves tip vortex towards to the shroud. The most important effect of squealer tip was delaying tip vortex at the rotor tip. The leakage flow is filled into the space between squealar and suction side of the rotor blade and released on the suction side at the mid chord location. Delaying tip vortex release to a chordwise location close to the trailing edge helps to direct tip vortex radially out. Further improvement can be obtained by increasing space between the squealer and suction side of the rotor tip by bending squealar extension towards to pressure side. A fully inclined squealer tip extension is designed by tilting the existing squealer extension about 25^o towards the pressure side. This inlined squealer design is shown in Figures 7 and 3e.

Figure 9 shows streamlines and stretched swirling strength

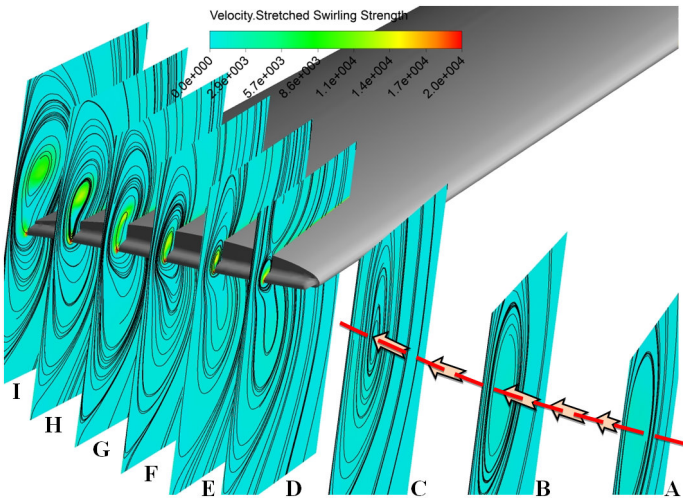

FIGURE 9. Blade tip constant circumferential angle planes drawn for "*inclined squealer*" tip extension with 3.04 % tip clearance

contour for inclined squealer tip extension. The leakage flow originating from the pressure side rolled up a small vortical structure between the inclined squealer and suction side. After plane G, the vortical structure appears near the suction side of the rotor tip. Tip leakage vortex originates starting from plane G and is directed towards shroud region.

OVERALL BENEFITS OF TIP TREATMENTS

Overall benefits gained from the tip treatments are analyzed by total pressure improvements in the stationary frame of reference. Table 1 shows computed thrust and ratio of "*leakage mass flow rate*" to the "*fan rotor mass flow rate*" for baseline rotor tips for two tip clearances and treated tips. The leakage mass flow rate is calculated on a plane that was defined between the rotor tip and shroud surface.

The result from the two tip clearances, tight (1.71 %) and coarse (3.04 %) are compared in Table 1. When the tip clearance decreased, the leakage mass flow rate also decreased and thrust was augmented. Decrease in leakage mass flow rate usually implies for an increase of overall mass flow rate passing from the duct.

The first two rows of Table 1 presents a comparison of both experimental and computational values of ducted fan thrust. The computational thrust results and measured values compare very well at two specific tip clearance values at 1.71 % and 3.04 %. All of the tip treatments shown in the Table 1 are computationally evaluated at the same tip clearance of 3.04 %. Aeromechanic and aerodynamic performance improvements provided by tip treatments are also tabulated in Table 1.

Figure 10 compares all of the tip treatments by comparing

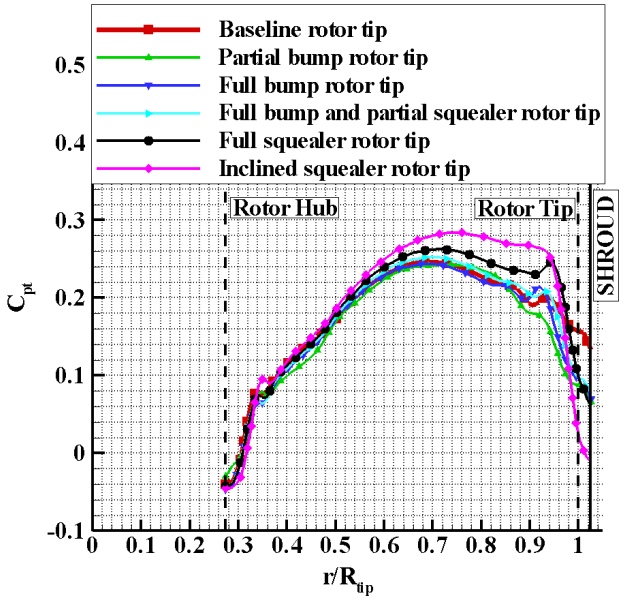

FIGURE 10. Comparison of computationally obtained total pressure distributions for all of the tip treatments and baseline rotor tip (3.04 % tip clearance).

the spanwise total pressure distributions in the stationary frame of reference. The computationally obtained total pressure distributions are drawn at the same rotor exit plane in which the baseline measurements are performed. This plane is located at about 45.72 mm downstream from the midspan of the fan rotor. The tip clearance value for all computations presented in Figure 8 is 3.04 %.

Because of the increased viscous losses induced at the rotor tip and radially tip leakage flow directed spanwise inward,

Ducted fan performance with baseline fan rotor tip				
	$\frac{\dot{m}_{leakage}}{\dot{m}_{fan}}$ (%)	Total Thrust (N)(Comp.)	Total Thrust (N) (Exp.)	ε (%)
Baseline rotor tip with 1.71 % t. c.	1.81	94.24	92.68	1.68
Baseline rotor tip with 3.04 % t. c.	3.41	85.16	83.55	1.93
Baseline rotor tip with 5.17 % t. c.	6.35	61.96	67.55	8.27

Ducted fan performance using treated fan rotor tips with 3.04 % tip clearance (Computational only)					
	$\frac{\dot{m}_{leakage}}{\dot{m}_{fan}}$ (%)	D. Thrust(N)	R. Thrust(N)	Total Thrust(N)	Thrust imp. (%)
Baseline rotor tip	3.41	27.20	57.96	**85.16**	—
Partial bump t.p.e.	3.58	26.68	54.06	**80.74**	-5.19
Full bump t.p.e.	3.28	26.70	58.20	**84.90**	-0.31
Full bump and par. squealer t.p.e.	2.86	27.66	58.68	**86.34**	1.37
Full squealer t.p.e.	2.41	30.50	59.81	**90.31**	6.04
Full inclined squealer t.p.e.	2.35	30.76	63.55	**94.31**	10.73

TABLE 1. Tip treatments and their computed performance in hover condition at 2400 rpm

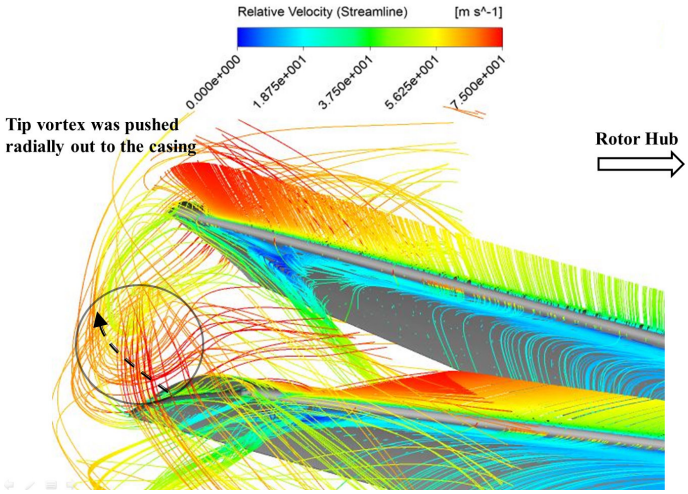

FIGURE 11. Streamlines around the "*inclined squealer*" rotor blade with 3.04 % tip clearance and rotor hub at 2400 rpm

the performance of partial and full tip platform extensions was lower than the baseline profile. Thrust obtained from the ducted fan was reduced for both treatments. Full tip platform extension combined with a partial squealar effectively reduced the tip leakage flow compared to partial and full tip platform extensions. However those of the gains provided by this treatment is not as high as the squealer tip treatments. Full squealer and inclined full squealers are the best performing ones. They are improving the aerodynamic performance by moving the tip vortex towards the shroud. Inclined squealer tip is increasing the thrust provided by the ducted fan by 10.73 % at hover condition 2400 rpm. It also decreases tip leakage mass flow rate at a considerable rate as shown in Table 1.

Figure 11 shows the streamlines drawn around the tip and mid-span regions for the fan rotor blade with inclined squealer tips. Streamlines are colored by relative velocity magnitude and drawn in the relative frame of reference. Inclined squealer tip directed tip leakage jet towards to the casing area by the as shown in Figure 11. As a result, the relative velocity magnitudes near the tip region and mid-span was increased due to the less interaction of leakage jet with the pressure side of the neighbouring blade.

EXPERIMENTAL VERIFICATION OF COMPUTATIONALLY DEVELOPED TIP CONCEPTS

Experimental Approach

The current study concentrates on the rotor tip section aerodynamic performance improvement by developing novel tip treatments. A computational model was used in the design and analysis of tip treatments as outlined in the previous sections. Selected treatments are tested using experimental methods. Experimental methods used for this research are total pressure survey at rotor exit, and aeromechanic measurements of the ducted fan system.

Fan rotor exit total pressure measurements in the stationary frame of reference were performed by using a Kiel total pressure probe. The Kiel total pressure probe having a 5 mm diameter total head was traversed in radial direction using a precision linear traverse mechanism controlled by a computer. The total pressure probe was always located 45.72 mm downstream of the fan rotor exit plane at 50% of blade span (mid-span). The Kiel probe was aligned with absolute rotor exit velocity at mid span position. Details of the probe alignment for different spanwise positions are explained in detail in the first part of this paper, [19].

Ducted fan aerodynamic research performed in this study requires high accuracy force and moment measurements. The 22" diameter fan is equipped with ATI-Delta six component force and torque transducer. Three components of force and three components of moments are measured. Part one of this paper explains the details of the force and torque measurement details and uncertainties.

Manufacturing Tip Platform Extensions Using a Stereolithography Based Rapid Prototyping Technique

In the previous sections, the computational analysis was performed for selecting the best tip profile geometries for improving aeromechanic and aerodynamic performance of the system. Squealer and inclined squealer tips were both improving thrust of the system while reducing leakage mass flow rate. They were also improving fan rotor exit total pressure distribution compared to baseline rotor tips. Three different squealer and inclined squealer designs were selected to be manufactured and experimentally tested in hover condition. The baseline tip clearance level for the computational analysis was 3.04 %. For the experimental program, squealer and inclined squealer tip treatments were designed for 3.04 %. Inclined squealer tip treatment was also tested for 5.17% tip clearance.

Selected tip shapes were designed as an extension to the tip of a baseline fan rotor tip. These extensions conformed to the external contour of the baseline tip section. Figure 12 shows drawings of the extensions designed for the baseline fan rotor tips. The extensions are glued to the top surface of the fan rotor blade using Cyanoacrylate that was having high viscosity and high impact strength. Figure 13 shows a rotor blade tip that has inclined squealer tip extension attached to it. Each tip concept tested had its own eight bladed rotor assembly. The tip clearance was measured from the base of the attached tip concept model as shown in Figure 13.

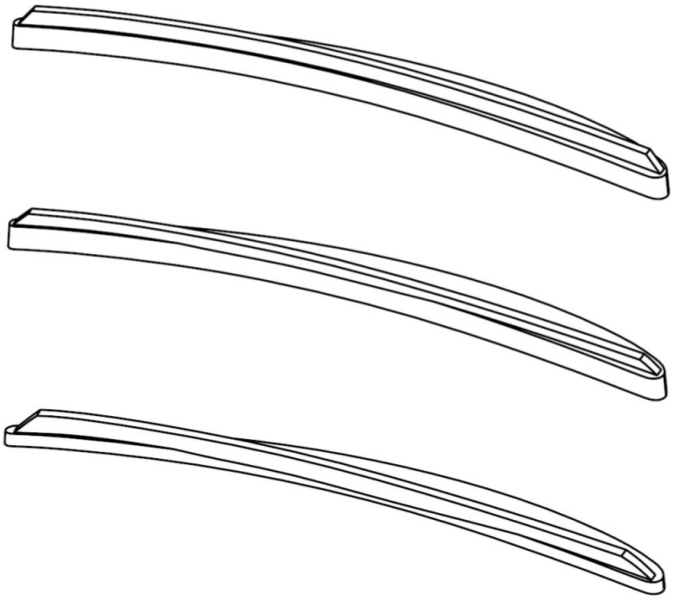

FIGURE 12. Squealer and inclined squealer tip extensions designed for SLA manufacturing (a) Squealer t.p.e.(3.04 % t.c.), (b) Inclined squealer t.p.e.(3.04 % t.c.), (c) Inclined squealer t.p.e.(5.17 % t.c.)

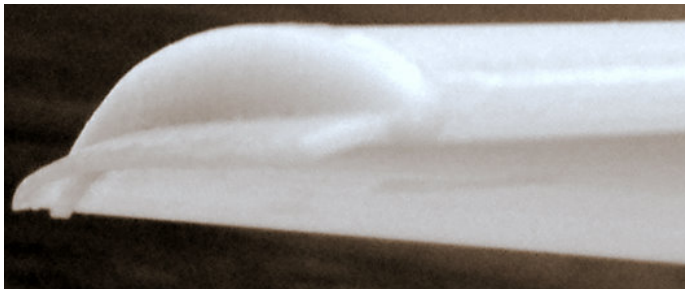

FIGURE 13. Inclined squealer t.p.e. applied to the rotor blade (5.17 % tip clearance)

Experimental Results

Force and Torque measurements Force and torque measurements for fan rotors with treated tips were performed in the 22" diameter axial flow fan research facility described in part one of this paper. Figure 14 shows measured thrust coefficient at various rotational speeds. The squealer and inclined tip squealer tip shapes were both augmenting thrust of the system compared to baseline rotor tip shapes. A maximum increase of 9.1 % was gained by using the squealar tip shape at 2700 rpm. The maximum increase in thrust gained by using inclined squealer tip was around 9.6 % 2700 rpm. Compared to computational results, experimental performance of squealer tips was better than computational performance in terms of measured thrust values. Using tip treatments improved performance of the baseline rotor tips with 3.04 % tip clearance such that the fan rotor with treated tips at the same tip clearance (3.04 %) performed almost as well as the baseline fan rotor performance having a tighter tip clearance (1.71 %), without any tip treatment. These comparisons are based on measured thrust in 22" diameter ducted fan research facility. The height of the squealer tips used in this study is always one fifth of the effective clearance t measured between the casing surface and the base platform of the blade tip.

Figure 15 illustrates the aeromechanic performance of inclined squealer at 5.17 % tip clearance compared to baseline rotor at the same clearance.When treatments were used with larger clearance, the improvements obtained was better. Total improvement in thrust was 15.9 % at 2700 rpm. Performance of the baseline rotor tips at 5.17 % tip clearance was enhanced so that they are almost performing like the 3.04 % tip clearance baseline rotor, without any tip treatment.

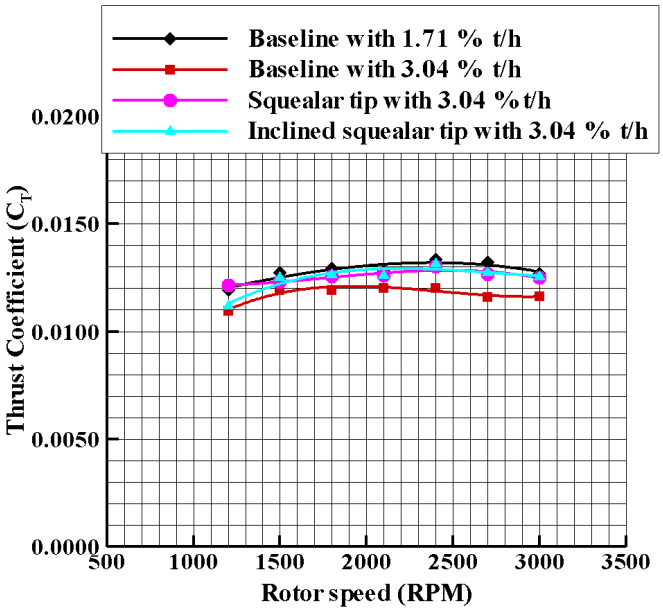

FIGURE 14. Measurements of thrust coefficient versus rotational speed for the rotor with squealer and inclined squealer tips at 3.04 % tip clearance

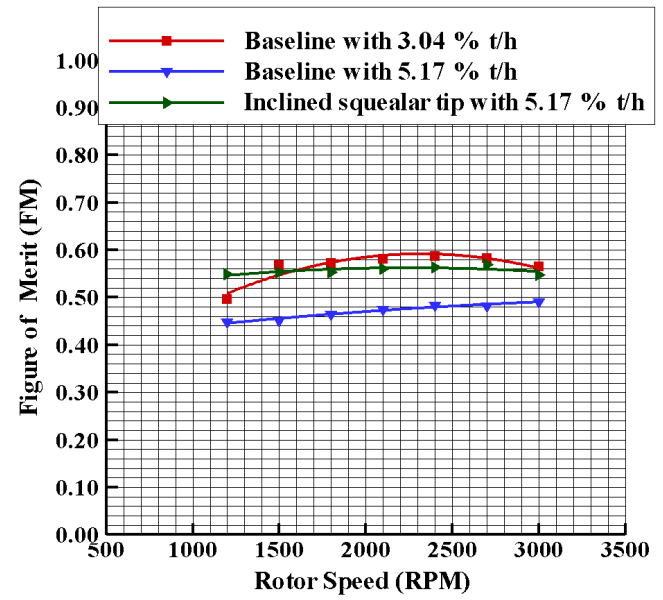

FIGURE 15. Measurements of thrust coefficient versus rotational speed for rotor with squealer and inclined squealer tips at 5.17 % tip clearance

Figures 16 and 17 illustrates the measured figures of merit plotted against the rotational speed of the fan rotor. Squealer

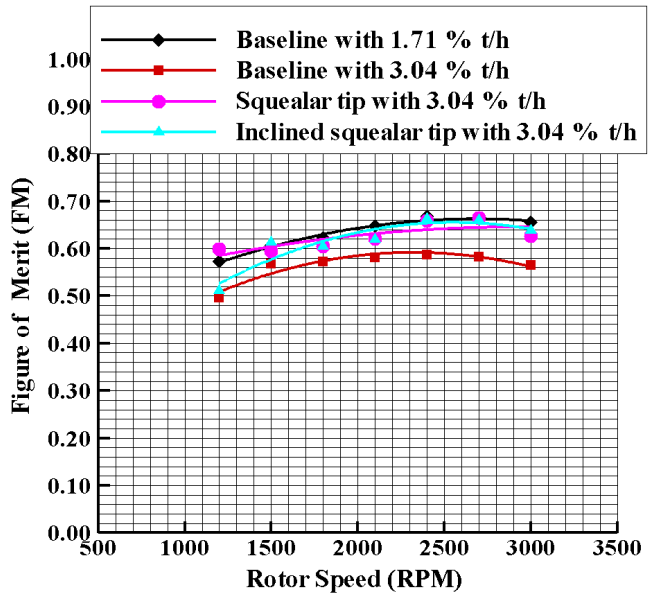

FIGURE 16. Measured figure of merit versus rotational speed for rotor with squealer and inclined squealer tips at 3.04 % tip clearance

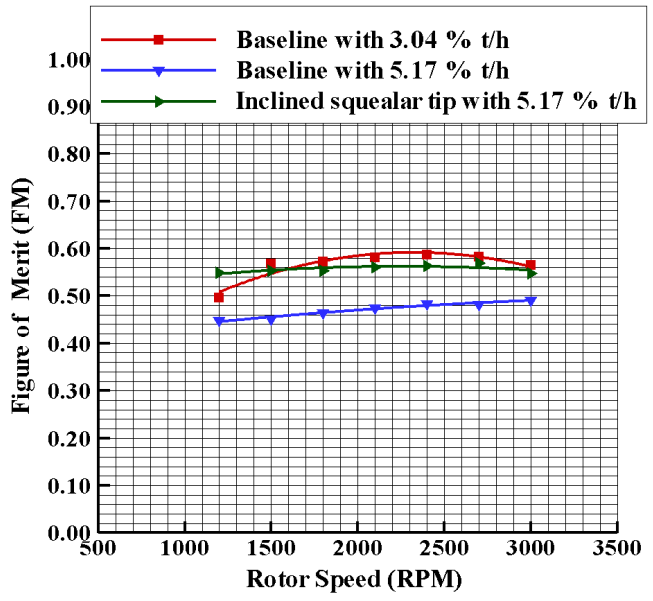

FIGURE 17. Measured figure of merit vs rotational speed for rotor with squealer and inclined squealer tips at 5.17 % tip clearance

and inclined squealer rotor tips increased hover efficiency compared to baseline rotor tips. Treated tip shapes at 5.17 % tip clearance are performing better than 3.04 % tip clearance (no tip treatments).

Total Pressure Measurements Aerodynamic performance of the ducted fan with squealer rotor tips was assessed by fan rotor exit total pressure measurements at hover condition. Figure 18 shows total pressure coefficient measured at fan rotor downstream from rotor hub to the shroud. It should be noted that there is almost no change in total pressure coefficient by using treated tips when $r/R_{tip} \leq 0.35$. Total pressure at the fan rotor exit plane is increased by using squealer and inclined squealer tip designs at 3.04 %tip clearance. Since the tip vortex that is originating from the rotor tip pressure side is repositioned by squealer and inclined squealer tips as mentioned in previous sections,total pressure distribution at the rotor tip where $r/R_{tip} \geq 0.3$ is enhanced. A significant portion of the blade span above $r/R_{tip} \geq 0.3$ starts producing a measurably higher total pressure as shown in Figure 18. The total pressure augmentation from the tip treatments are particularly effective near the blade tip where $r/R_{tip} \geq 0.85$. For the larger tip clearace 5.17 %, using inclined squealer tip also improved the total pressure distribution near the rotor tip region and performed better than the smaller tip clearance baseline tip performance at 3.04 %.

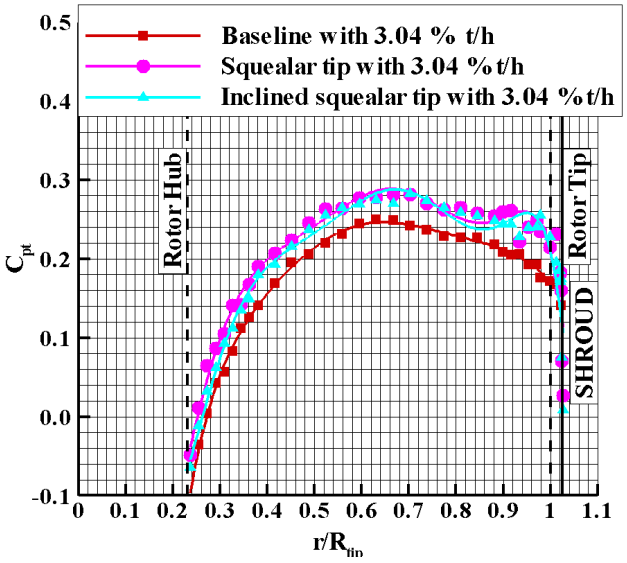

FIGURE 18. Total pressure measured at downstream of the rotor at 2400 rpm for squealer tips wit 3.04 % tip clearence

CONCLUSIONS

This paper presents a set of comprehensive ducted fan aerodynamic measurements validating and supporting the computationally developed novel tip treatments. The new tip treatments are referred as full and partial bump tip extensions, full bump and partial squealar tip extensions, and full squealer and inclined squealer tips.

The losses generated were highly related to the tip vortex traveling direction an trajectory. If the tip vortex traveled radially inward, then the losses related to the blockage effect influenced a larger portion of the blade span and the rotor tip stall was more pronounced.

The current study used squealer heights that have a total height of one fifth of the effective clearance t between the base platform and the casing. A full squealer rotor tip was effective in changing the direction of the tip vortex. The tip vortex was pushed radially out to the casing area. The computational results showed that the squealer tip successfully blocked the tip vortex between leading edge and mid-chord of the rotor tip profile.

An inclined full squealer tip was also conceived to move tip vortex origination location closer to the trailing edge. This is achieved by allocating more space to the tip vortex to fill between squealer and suction side of the rotor tip.

Overall aeromechanic performance gains obtained by using tip platform extensions were assessed the from computations. Pressure side tip platform extensions reduced thrust obtained from the ducted fan.

The best performing profiles were full and inclined full squealer extensions. Both experimental measurements and

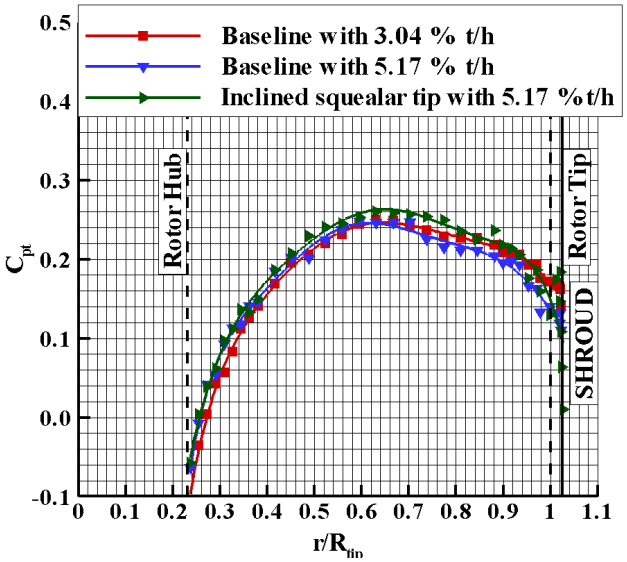

FIGURE 19. Total pressure measured at downstream of the rotor at 2400 rpm for squealer tips wit 5.17 % tip clearence

computations confirmed this observation. Full squealer tip extension increased thrust of the ducted fan by 6.04 % and reduced the leakage mass flow rated by 29.3 % compared to the baseline rotor tips. Inclined squealer tips increased the thrust by

10.73 % while reducing the leakage mass flow rate by 31.0 % .

Experimental investigation was also performed by manufacturing squealer and inclined squealer tip extensions for 3.04 % tip clearance and inclined squealer tip extensions for 5.17 % tip clearance. Solid models of tip extension pieces originally developed for computational purposes were directly used to manufacture experimental tip treatment models in a rapid prototyping process.

Aeromechanic and aerothermodynamic measurements showed that using full inclined squealer tips with 5.17 % tip clearance is equivalent to working with a 3.04 tip clearance baseline rotor.

The squealar and inclined squealer tips at 3.04 % tip clearance also improved performance of the fan rotor. This operation was equivalent to working with a baseline rotor at 1.71 % tip clearance. This feature of the tip treatments allows using treated rotor blades at larger clearances while performing as well as the operating at much smaller clearances.

The novel tip treatments filling the one fifth of the effective gap between the tip platform and the casing can easily be manufactured out of attachable and flexible materials for VTOL UAV fan implementation. The current state of the art in SLA manufacturing allows the rapid production of the proposed tip treatments out of materials such as rubber or other flexible plastic materials of resilient character.

While the flexible tip treatments improve ducted fan thrust and reduce tip clearance leakage mass flow rate, they can be quickly replaced in case of a rubbing incident during the field operation.

ACKNOWLEDGMENT

The authors acknowledge the financial support provided by the PSU Vertical Lift Center of Excellence (VLRCOE)and National Rotorcraft Technology Center (NRTC) (Under U.S. Army Research Office grant # W911W6-06-2-0008). They wish to thank to Ozhan Turgut for his support throughout this effort. They are also indebted to Mr. Harry Houtz for his technical support.

REFERENCES

[1] Lee, G. H., Baek, J. H., and Myung, H. J., 2003. "Structure of tip leakage in a forward-swept axial-flow fan". *Flow, Turbulence and Combustion,* ***70***, pp. 241–265.

[2] Jang, C. M., Furukawa, M., and Inoue, M., 2001. "Analysis of vortical flow field in a propeller fan by ldv measurements and les - parts i, ii". *Journal of Fluids Engineering,* ***123***, pp. 748–761.

[3] Storer, J. A., and Cumpsty, N. A., 1991. "Tip leakage flow in axial compressors". *Journal of Turbomachinery,* ***113***, April.

[4] Lakshminarayana, B., Zaccaria, M., and Marathe, B., 1995. "The structure of tip clearance flow in axial flow compressors". *Journal of Turbomachinery,* ***117***, pp. 336–347.

[5] Matzgeller, R., Bur, P., and Kawall, J., 2010. "Investigation of compressor tip clearance flow structure". *Proceedings of ASME Turbo Expo 2010:Power for Land, Sea and Air,* ***GT2010-23244***.

[6] Inoue, M., Kuroumaru, M., and Furukawa, M., 1986. "Behavior of tip leakage flow behind an axial compressor rotor". *Journal of Gas Turbine and Power,* ***108***, pp. 7–14.

[7] Furukawa, M., Inoue, M., Kuroumaru, M., Saik, i. K., and Yamada, K., 1999. "The role of tip leakage vortex breakdown in compressor rotor aerodynamics". *Journal of Turbomachinery,* ***121***, pp. 469–480.

[8] Fujita, H., and Takata, H., 1984. "A study on configurations of casing treatment for axial flow compressors". *Bulletin of the JSME,* ***27***, pp. 1675–1681.

[9] Moore, R. D., Kovich, G., and Blade, R. J., 1971. Effect of casing treatment on overall and blade-element performance of a compressor rotor. Tech. Rep. TN-D6538, NASA.

[10] Corsini, A., Perugini, B., Rispoli, F., Kinghorn, I., and Sheard, A. G., 2006. "Investigation on improved blade tip concept". *ASME Paper*(GT2006-90592).

[11] Corsini, A., Rispoli, F., and Sheard, A. G., 2006. "Development of improved blade tip end-plate concepts for low-noise operation in industrial fans". *Proceedings of Conference on Modeling Fluid Flows CMMF06*.

[12] Corsini, A., Perugini, B., Rispoli, F., Kinghorn, I., and Sheard, A. G., 2007. "Experimental and numerical investigations on passive devices for tip-clearance induced noise reduction in axial flow fans". *Proceedings of the 7th European Conference on Turbomachinery*.

[13] Corsini, A., Perugini, B., Rispoli, F., Sheard, A. G., and Kinghorn, I., 2007. "Aerodynamic workings of blade tip end-plates designed for low-noise operation in axial flow fans". *ASME Paper*(GT2007-27465).

[14] Alessandro, C., Franco, R., and Sheard, A. G., 2010. "Shaping of tip end-plate to control leakage vortex swirl in axial flow fans". *Journal of Turbomachinery,* ***132***(3).

[15] Wisler, D., 1985. "Tip clearance effects in axial turbomachines". *Von Karman Institute for fluid dynamics Lecture Series*(5).

[16] Akturk, A., and Camci, C., 2010. "Axial flow fan tip leakage flow control using tip platform extensions". *J. Fluids Eng.,* ***132***(5).

[17] Martin, P. B., and Boxwell, D. A., 2005. "Design, analysis and experiments on a 10-inch ducted rotor vtol uav". *AHS International Specialists Meeting on Unmanned Rotorcraft: Design, Control and Testing*.

[18] Martin, P., and Tung, C., 2004. "Performance and flowfield measurements on a 10-inch ducted rotor vtol uav". *60th Annual Forum of the American Helicopter Society*.

[19] Akturk, A., and Camci, C., 2011. "Tip clearance investigation of a ducted fan used in vtol uavs part 1: Baseline experiments and computational validation". *Proceedings of ASME Turbo Expo 2011:Power for Land, Sea and Air,* ***GT2011-46356***.